Constraints from the CMB temperature and other common observational data-sets on variable dark energy density models

Philippe Jetzer[1*] and Crescenzo Tortora[1†]
[1] *Universität Zürich, Institut für Theoretische Physik, Winterthurerstrasse 190, CH-8057, Zürich, Switzerland*

The thermodynamic and dynamical properties of a variable dark energy model with density scaling as $\rho_x \propto (1+z)^m$, z being the redshift, are discussed following the outline of Jetzer et al. [1]. This kind of models are proven to lead to the creation/disruption of matter and radiation, which affect the cosmic evolution of both matter and radiation components in the Universe. In particular, we have concentrated on the temperature-redshift relation of radiation, which has been constrained using a very recent collection of cosmic microwave background (CMB) temperature measurements up to $z \sim 3$. For the first time, we have combined this observational probe with a set of independent measurements (Supernovae Ia distance moduli, CMB anisotropy, large-scale structure and observational data for the Hubble parameter), which are commonly adopted to constrain dark energy models. We find that, within the uncertainties, the model is indistinguishable from a cosmological constant which does not exchange any particles with other components. Anyway, while temperature measurements and Supernovae Ia tend to predict slightly decaying models, the contrary happens if CMB data are included. Future observations, in particular measurements of CMB temperature at large redshift, will allow to give firmer bounds on the effective equation of state parameter $w_{\rm eff}$ of this kind of dark energy models.

PACS numbers: 98.80.-k, 95.36.+x, 05.70.-a
Keywords: Cosmology, Dark energy, Thermodynamics

I. INTRODUCTION

The current standard cosmology model relies on the existence of two unknown dark components, the so called "dark matter" (DM) and "dark energy" (DE), which amount to $\sim 25\%$ and $\sim 70\%$ of the total energy budget in the Universe, respectively. According to several observations, the Universe is spatially flat and in an accelerated phase of its expansion [2–6]. DE, described as a cosmological constant Λ in its simplest form, is modelled by a fluid with a negative pressure, which is a fundamental ingredient to explain the actual accelerated expansion of the Universe.

Several models have been proposed to explain DE [7–14]. An alternative consists to consider a phenomenological variable DE density with continuous creation/disruption of photons [1, 15–18] or matter [19, 20]. The DE might decay/grow slowly in the course of the cosmic evolution and thus provide the source/sink term for matter and radiation. Different such models have been discussed and strong constraints come from very accurate measurements of the cosmic microwave background (CMB) radiation and other typical cosmological probe.

CMB radiation is the best evidence for an expanding Universe starting from an initial high density state. Within the Friedmann-Robertson-Walker (FRW) models of the Universe the radiation, after decoupling, expands adiabatically and scales as $(1+z)$, z being the redshift [21]. If we assume that each component is not conserved, contrarily to the standard scenario, then depending on the decay mechanism of the DE, the created photons could lead to distortions in the Planck spectrum of the CMB, and change the evolution of its temperature. The chance to appreciate the deviation from the standard temperature evolution is given by the increasingly number of recent works collecting observations of CMB temperature both at low [22, 23] and higher redshifts [24].

Following the theoretical lines of [15–18], in Jetzer et al. [1] we have discussed a variable DE model $\Lambda(z) \propto (1+z)^m$ decaying into photons and DM particles. In particular we studied thermodynamical aspects in the case of a continuous photon creation, which implies a modified temperature redshift relation for the CMB. We have tested the predicted temperature evolution of radiation with some recent data on the CMB at higher redshift from both Sunyaev-Zel'dovich (SZ) effect and high-redshift QSO absorption lines.

In this paper we will present the results obtained in [1] within a more detailed theoretical background, by further discussing the main hypothesis which concern the energy conservation and thermodynamical laws. Furthermore, we will test our model with an updated collection of data, joining our sample with the new temperature observations reported in [24]. For the first time we will combine to the temperature measurements also the data from different kind of observations, like distance moduli of Supernovae Ia, observations of the CMB anisotropy and the large-scale structure, together with observational Hubble parameter estimations. We will dedicate a particular attention to the estimate of both the actual matter

*jetzer@physik.uzh.ch
†ctortora@physik.uzh.ch

density parameter, the DE parameter m and the effective equation of state parameter $w_{\rm eff}$. The impact of each observational probe on these estimates is also investigated.

The paper is organised as follows. In §II we will present the model, while the data sets and fitting procedure are described in §III. The results are discussed in §IV and §V is devoted to a discussion of the results and conclusions.

II. THEORETICAL FRAMEWORK

A. Friedmann equations

We assume a cosmological framework based on the usual Robertson-Walker (RW) metric element [21] and that the Universe contains three different components: a) a matter (both baryons and DM) fluid, with equation of state $p_m = 0$ (since $p_m << \rho_m$), b) a generalised fluid with pressure $p_\gamma = (\gamma-1)\rho_\gamma$, where γ is a free parameter, which is set to 4/3 for a properly said radiation fluid, and c) a DE, x component, with pressure p_x and density ρ_x. The equation of state for the x component could assume a very general expression, but we limit ourselves to consider the simple linear relation $p_x = w_x\rho_x$. We will set any 'bare' cosmological constant Λ_0 equal to 0 [1]. With these components we get for the Einstein field equations [21]

$$8\pi G\rho_{tot} = 3\frac{\dot{R}^2}{R^2} + 3\frac{k}{R^2} \ , \tag{2.1}$$

$$8\pi G p_{tot} = -2\frac{\ddot{R}}{R} - \frac{\dot{R}^2}{R^2} - \frac{k}{R^2} \ , \tag{2.2}$$

where $p_{tot} = p_\gamma + p_x$ and $\rho_{tot} = \rho_m + \rho_\gamma + \rho_x$ are the total pressure and density, R is the scale factor, $k = 0, \pm 1$ is the curvature parameter and a dot means time derivative. Furthermore, we will assume that there is no curvature, thus $k = 0$ [4].

In the following we will adopt $w_x = -1$, however since we are assuming that the vacuum decays into radiation and massive particles, the effective equation of state w_{eff}, which is the measured quantity, can differ from -1 (see later for further details).

B. Cosmological conservation laws and density evolution

Following Jetzer et al. [1] (but see also [15, 17]) we set here the energy conservation equation for the different fluids. The fluid as whole, verifies the Bianchi identity, which means that energy and momentum are locally conserved. In formulae it is $\nabla_\mu T^{\mu\nu} = 0$, with $T^{\mu\nu}$ the stress-energy tensor

$$T^{\mu\nu} = (\rho_{tot} + p_{tot})u^\mu u^\nu - p_{tot} g^{\mu\nu} \tag{2.3}$$

with u^μ being the four velocity. After easy calculations, this conservation law reads

$$\dot{\rho}_{tot} + 3(\rho_{tot} + p_{tot})H = 0 \ , \tag{2.4}$$

where $H = \dot{R}/R$ is the Hubble parameter. In the standard approach, each component is conserved, thus Eq. (2.4) holds for all the fluid components, but here we will suppose that each component will exchange energy with each other. In particular, for matter, radiation and DE we impose the following relations (see also [25])

$$\dot{\rho}_m + 3\rho_m H = (1-\epsilon)\ C_x \ , \tag{2.5}$$

$$\dot{\rho}_\gamma + 3\gamma\rho_\gamma H = \epsilon\ C_x \ , \tag{2.6}$$

$$\dot{\rho}_x + 3(p_x + \rho_x)H = -C_x \ , \tag{2.7}$$

where we assume that both the matter and the radiation fluids exchange energy with the DE as parameterized by C_x and ϵ. In particular, C_x depends on the DE and, indeed, acts as a source/sink term for the fluids energy. Evidently, if no interaction between the different components exists, then C_x is null and the standard picture is recovered. Moreover, if $\epsilon = 0$ ($\epsilon = 1$), then the DE exchanges all the energy with matter (radiation). C_x can describe different physical situations such as, for instance, a thermogravitational quantum creation theory [16] or a quintessence scalar field cosmology [8]. As we will discuss later on, ϵ has to be very small (i.e., $\epsilon \ll 1$), otherwise the radiation density would become much too big, contrary to present values. As an order of magnitude estimate we expect $\epsilon \simeq \frac{p_\gamma+\rho_\gamma}{\rho_m}$, for which indeed $\epsilon \ll 1$, since $p_\gamma + \rho_\gamma \ll \rho_m$.

Adopting as mentioned above the relation $p_x = -\rho_x$ and defining $\rho_x = \Lambda(t)/(8\pi G)$, from Eq. (2.7) we obtain

$$C_x = -\frac{\dot{\Lambda}(t)}{8\pi G} \ . \tag{2.8}$$

We assume a power law model for the $\Lambda(t)$ function, $\Lambda(t) = B(R/R_0)^{-m}$, or equivalently in terms of redshift, $\Lambda(z) = B(1+z)^m$, where B is a constant. The value of this constant is $B = 3H_0^2(1-\Omega_{\rm m0})$, which can be found using Eq. (2.1) at the present epoch, assuming that today $\rho_\gamma \ll \rho_m, \rho_x$. Thus, the density evolution for the x component is given by

$$\rho_x/\rho_{crit} = (1-\Omega_{\rm m0})(1+z)^m, \tag{2.9}$$

where we have defined as $\rho_{crit} = \frac{3H_0}{8\pi G}$ the present critical density of the Universe. If m is positive, then the DE slowly decreases as a function of the cosmic time, whereas if m is negative the inverse process happens.

From Eqs. (2.5) and (2.6) we derive the evolution laws for matter and radiation,

$$\rho_m/\rho_{crit} = \Omega_{\rm m0}(1+z)^3 - (1-\epsilon)\frac{m(1-\Omega_{\rm m0})}{m-3}[(1+z)^m - (1+z)^3] \ , \tag{2.10}$$

$$\rho_\gamma/\rho_{crit} = \Omega_{\gamma 0}(1+z)^{3\gamma} - \epsilon\frac{m(1-\Omega_{\rm m0})}{m-3\gamma}[(1+z)^m - (1+z)^{3\gamma}] \ , \tag{2.11}$$

where $\Omega_{\rm m0}$ and $\Omega_{\gamma 0}$ are the matter and radiation energy densities at $z=0$, respectively.

Since we are interested in the evolution of the radiation temperature, it is useful to discuss the extreme case when only photons enter in the process (i.e. $\epsilon = 1$). Then for the matter density in Eq. (2.10) the usual evolution $\propto (1+z)^3$ holds, while the radiation besides the usual term $\Omega_{\gamma 0}(1+z)^{3\gamma}$ has also a perturbative term depending on m. Since today [1] $\Omega_{\gamma 0} \sim 5\times 10^{-5}$ it turns out that m has to be extremely small $\lesssim 10^{-4}$. Therefore, unless m is extremely small or vanishing, DE has to decay mainly in matter with possibly some photons as well. Thus the condition $\epsilon \ll 1$ has to hold.

C. Hubble and deceleration parameter

Due to the very small value of $\Omega_{\gamma 0}$ it follows that the evolution of the Universe is essentially driven by the DE and DM, therefore, from Eq. (2.1) the following law for the Hubble parameter holds

$$H(z) \simeq \frac{8\pi G}{3}(\rho_m + \rho_x) = H_0\left[\frac{3(1-\Omega_{\rm m0})}{3-m}(1+z)^m + \frac{(3\Omega_{\rm m0}-m)}{3-m}(1+z)^3\right]^{1/2} , \tag{2.12}$$

which is obviously the same expression found in Ma [20].

Recasting Eq. (2.7), it is possible to write

$$\dot\rho_x + 3H(p_x + \rho_x + \frac{C_x}{3H}) = 0 \ , \tag{2.13}$$

which shows that the term C_x contributes to an effective pressure

$$p_{\rm eff} = p_x + \frac{C_x}{3H} = -\rho_x + \frac{C_x}{3H} \ . \tag{2.14}$$

Therefore, we get an equivalent effective DE equation of state $w_{\rm eff}$ [20]

$$w_{\rm eff} = \frac{p_{\rm eff}}{\rho_x} = \frac{m}{3} - 1. \tag{2.15}$$

If $m > 0$ then we have $w_{\rm eff} > -1$, i.e. our model is quintessence-like [7, 8, 13], while we have a phantom-like [10] model when m is negative and $w_{\rm eff} < -1$. Another interesting quantity is the deceleration parameter, which can be written as

$$q(z) = -\frac{\ddot R R}{\dot R^2} = \frac{(1+z)^3(m-3\Omega_{\rm m0}) + 3(m-2)(1+z)^m(\Omega_{\rm m0}-1)}{2(1+z)^3(m-3\Omega_{\rm m0}) + 6(1+z)^m(\Omega_{\rm m0}-1)} \ . \tag{2.16}$$

Imposing that $q(z)=0$, we can determine the *transition redshift*, i.e. the redshift at which the Universe changed from a deceleration to an acceleration phase, which is given by

$$z_T = \left(\frac{3(2-m)(1-\Omega_{\rm m0})}{3\Omega_{\rm m0}-m}\right)^{\frac{1}{3-m}} - 1 \ . \tag{2.17}$$

From this result we see that the larger m is, the earlier the Universe changes from deceleration to acceleration.

D. Thermodynamical aspects and CMB temperature evolution

We follow here the approach outlined in Lima [15], where he defines a current as $N^\alpha = nu^\alpha$ with n being the particle number density of the photons or of the DM particles. Indeed, there is a current for each of these components. Due to the decaying vacuum the current satisfies the following balance equation (one for each component)

$$\dot n_i + 3n_iH = \psi_i \ , \tag{2.18}$$

with $i = \gamma$ or DM (γ for the photons and DM for the dark matter) and ψ_i is the corresponding particle source. For decaying vacuum models $\psi_\gamma + \psi_{DM}$ is positive and related to the rate of change of ρ_x. We can also define an entropy current of the form

$$S^\alpha = \sum_i n_i\sigma_i u_i^\alpha \ , \tag{2.19}$$

where σ_i is the specific entropy per particle (photons, DM and in principle also DE). If the DE ρ_x is constant the above entropy current is conserved. The existence of a non equilibrium decay process of the vacuum implies $S^\alpha_{;\alpha} \geq 0$, thus an increase of the entropy as a consequence of the second law of thermodynamics. In principle the second law should be applied to the system as a whole, thus including the vacuum component [25]. Assuming that the vacuum is like a condensate with zero chemical potential μ_{vac} it follows from Euler's relation

$$\mu_{vac} = \frac{\rho_x + p_x}{n} - T\sigma_{vac} \ , \tag{2.20}$$

provided $w_x = -1$, that $\sigma_{vac} = 0$ and thus its contribution to the entropy current vanishes. Given our assumptions the vacuum plays the role of a condensate carrying no entropy.

[1] The present radiation density is the only cosmological parameter accurately measured. The radiation density is dominated by the energy in the cosmic microwave background (CMB), and the COBE satellite FIRAS experiment determined its temperature to be $T = 2.725 \pm 0.001\ K$ [26], corresponding to $\Omega_{\gamma 0} \sim 5\times 10^{-5}$.

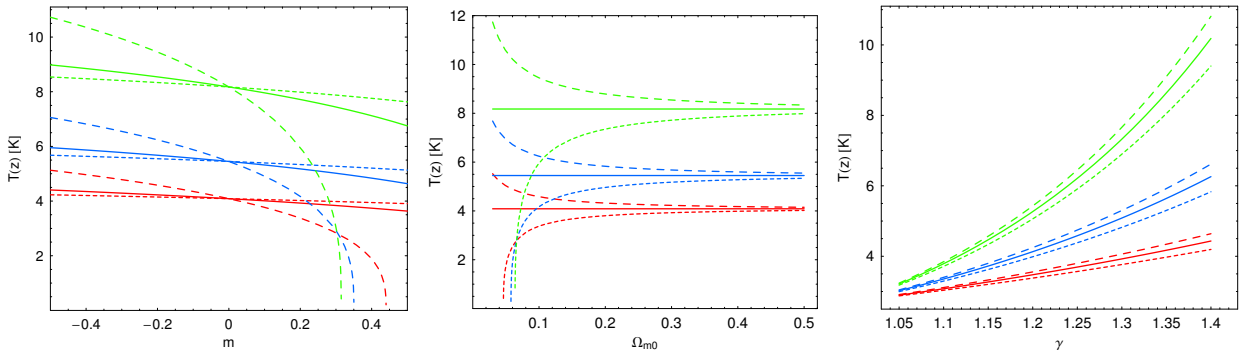

FIG. 1: Radiation temperature in Eq. (2.33) in terms of m, $\Omega_{\rm m0}$ and γ. Red, blue and green lines are for $z = 0.5$, $z = 1$ and $z = 2$, respectively. *Left.* T as a function of m. $\gamma = 4/3$ and $\Omega_{\rm m0} = 0.1$ (long-dashed), $= 0.3$ (continue) and $= 0.5$ (short-dashed). *Middle.* T as a function of $\Omega_{\rm m0}$. $\gamma = 4/3$ and $m = -0.2$ (long-dashed), $= 0$ (continue) and $= 0.2$ (short-dashed). *Right.* T as a function of γ. $\Omega_{\rm m0} = 0.273$ and $m = -0.2$ (long-dashed), $= 0$ (continue) and $= 0.2$ (short-dashed).

For instance, for quintessence models in the limit where the scalar field does not depend on time, and thus its time derivative vanishes, one gets $w_x = -1$. In the later stages of the Universe the time dependence is possibly very weak so that $w_x = -1$ holds up to small corrections.

The equation for the particle number density of radiation component is given by Eq. (2.18) with $i = \gamma$. Using Gibbs law and well-known thermodynamic identities, following the derivation given in the paper by Lima et al. [17], one gets (see also [1, 15])

$$\frac{\dot{T}}{T} = \left(\frac{\partial p_\gamma}{\partial \rho_\gamma}\right)_n \frac{\dot{n}_\gamma}{n_\gamma} - \frac{\psi_\gamma}{n_\gamma T \left(\frac{\partial \rho_\gamma}{\partial T}\right)_n}\left[p_\gamma + \rho_\gamma - \frac{n_\gamma \epsilon\, C_x}{\psi_\gamma}\right] . \tag{2.21}$$

To get a black-body spectrum the second term in brackets in Eq. (2.21) has to vanish, thus

$$\epsilon\, C_x = \frac{\psi_\gamma}{n_\gamma}\left[p_\gamma + \rho_\gamma\right] . \tag{2.22}$$

Thus, Eq. (2.21) becomes

$$\frac{\dot{T}}{T} = \left(\frac{\partial p_\gamma}{\partial \rho\gamma}\right)_n \frac{\dot{n}_\gamma}{n_\gamma} . \tag{2.23}$$

With $\left(\frac{\partial p_\gamma}{\partial \rho_\gamma}\right)_n = (\gamma - 1)$ one obtains

$$\frac{\dot{T}}{T} = (\gamma - 1)\frac{\dot{n}_\gamma}{n_\gamma} . \tag{2.24}$$

Using the equation for the particle number conservation Eq. (2.18) into Eq. (2.24) leads to

$$\frac{\dot{T}}{T} = (\gamma - 1)\left[\frac{\psi_\gamma}{n_\gamma} - 3H\right] . \tag{2.25}$$

With Eqs. (2.22) and (2.25) we get

$$\frac{\dot{T}}{T} = (\gamma - 1)\left[-\frac{\epsilon\,\dot{\Lambda}}{8\pi G(p_\gamma + \rho_\gamma)} - 3H\right] . \tag{2.26}$$

Now, following the previous discussion on ϵ and aiming to be very general, we set $\epsilon = \frac{\rho_\gamma + p_\gamma}{\rho_m}\tilde{\epsilon}$, where $\tilde{\epsilon}$ is a new parameter and insert it into Eq. (2.26). Taking the sum of Eqs. (2.1) and (2.2) we find

$$8\pi G(\rho_{tot} + p_{tot}) \simeq 8\pi G\rho_m = 2\frac{\dot{R}^2}{R^2} - 2\frac{\ddot{R}}{R} = -2\dot{H} . \tag{2.27}$$

Finally, we obtain the expression

$$\frac{\dot{T}}{T} = (\gamma - 1)\left[\frac{\dot{\Lambda}\tilde{\epsilon}}{2\dot{H}} - 3H\right] , \tag{2.28}$$

which we can integrate

$$\int_{t_1}^{t_0} \frac{\dot{T}}{T} dt = (\gamma - 1)\int_{t_1}^{t_0}\left[\frac{\dot{\Lambda}\tilde{\epsilon}}{2\dot{H}} - 3H\right] dt , \tag{2.29}$$

where t_0 denotes the present time and t_1 some far instant in the past. Indeed, if $\dot{\Lambda}$ vanishes and $\gamma = 4/3$ one gets the usual dependence $T(t) = \frac{R(t_1)T(t_1)}{R(t)}$ for a radiation fluid. To carry out the integration of the first term on the right hand side it is useful to perform a change of variable from t to z and accordingly $\frac{dt}{dz} = \frac{-1}{H(1+z)}$. This way we get (with z_1 corresponding to the time t_1 and $z_0 = 0$ corresponding to t_0 present time)

$$ln\frac{T(z=0)}{T(z_1)} + 3(\gamma - 1)ln\frac{R(z=0)}{R(z_1)} = \frac{(\gamma - 1)}{2}\int_0^{z_1}\frac{\Lambda'\tilde{\epsilon}}{H'H(1+z)}dz , \tag{2.30}$$

where $'$ denotes derivative with respect to z.

As next we insert $H(z)$ and its derivative as taken from Eq. (2.12) into Eq. (2.30) and integrate it, to get (setting $z_1 = z$)

$$T(z) = T_0 \left(\frac{R_0}{R(z)}\right)^{3(\gamma-1)} exp\left(\frac{B(1-\gamma)\tilde{\epsilon}}{3H_0^2(\Omega_{\rm m0}-1)}A\right) , \tag{2.31}$$

where

$$A = ln((m-3\Omega_{\rm m0}) + m(1+z)^{m-3}(\Omega_{\rm m0}-1)) \\ -ln((m-3)\Omega_{\rm m0})] . \tag{2.32}$$

We can also write Eq. (2.31) as

$$T(z) = T_0(1+z)^{3(\gamma-1)} \\ \times \left(\frac{(m-3\Omega_{\rm m0}) + m(1+z)^{m-3}(\Omega_{\rm m0}-1)}{(m-3)\Omega_{\rm m0}}\right)^{\tilde{\epsilon}(\gamma-1)} . \tag{2.33}$$

We inserted in the exponent of Eq. (2.31) the explicit form of B, thus getting as exponent in the above Eq. $\tilde{\epsilon}(\gamma-1)$. Hereafter, we will set $\tilde{\epsilon}=1$. Clearly $\tilde{\epsilon}$ and m are not independent, we checked using the temperature redshift data that if $\tilde{\epsilon}$ is bigger (~ 10 or more), then m has to be extremely small consistently with what mentioned in section II.B (as it would lead to a too high production of photons in the DE decay). On the other hand, if $\tilde{\epsilon}$ gets smaller (e.g., ~ 0.1) m gets bigger (~ 0.2) and accordingly w_{eff}, moreover m would be poorly constrained, since the uncertainties would then be very high. But from the other data (without the the temperature ones) there are already stringent limits on m and thus this way one could get lower limits on $\tilde{\epsilon}$, under the assumption that DE decays also in photons.

Notice that for $z=0$ we have $T(0)=T_0$, whereas for $m=0$ the expression in the parenthesis is equal to 1 and thus $T(z)=T_0(1+z)^{3(\gamma-1)}$, which for the canonical value of $\gamma = 4/3$ reduces to the standard expression.

In Fig. 1, the temperature relation from Eq. (2.33) is discussed in terms of the model parameters and redshift. At fixed redshift, the temperature is a decreasing function of m, i.e. larger m means a colder CMB radiation temperature and when compared with the unperturbed case with $m=0$, then a decaying/increasing model predicts colder/hotter temperatures. The temperature is sensitive to $\Omega_{\rm m0}$ mainly at $\Omega_{\rm m0} \lesssim 0.1-0.2$ and less at larger $\Omega_{\rm m0}$, while it is a strong function of γ, increasingly as a function of redshift.

III. FITTING PROCEDURE AND DATA

To constrain the parameters of the model we use a set of different kinds of measurements. Our data sets include the measurements of CMB temperatures from high redshift quasars and SZ effect, high quality "UnionII" SN Ia data, baryon acoustic oscillation measurement from the Sloan Digital Sky Survey, the shift parameter from WMAP three years results and 9 observational $H(z)$ data. To break the degeneracies between the parameters and explore the power and differences of the constraints for these data sets, we use them in several combinations to perform our fitting.

In order to constrain the model parameters we maximize the likelihood function $\mathcal{L}(\mathbf{p}) = \exp\left[-\frac{1}{2}\chi^2\right]$, where $\mathbf{p}$ denotes the set of model parameters and χ^2 is a suitable merit function[2]. The isolikelihood (or the isoχ^2) contours provide constraints on the parameter space. The 68% confidence levels (CL) are obtained by imposing $\Delta\chi^2 = \chi^2 - \chi^2_{min} = 1$ and 2.3 for $n_p = 1$, 2 free parameters, where χ^2_{min} is the minimum of χ^2 function. The 90% CL, is given by $\Delta\chi^2 = 2.71$ and 4.61 for $n_p = 1$, 2. Finally, the 95% CL is given by $\Delta\chi^2 = 4$ and 6.17 for $n_p = 1$, 2. In order to give a quantification of the errors on a given parameter we can follow different approaches. When $n_p = 1$, then the error on the parameter is determined simply adopting the above conditions on $\Delta\chi^2$. On the contrary, if $n_p = 2$ (which is one of the cases we will investigate in the paper), to constrain a given parameter p_1, we rely on the marginalized function defined as $\mathcal{L}_{p_1}(p_1) \propto \int_{p_2} dp_2 \mathcal{L}(\mathbf{p})$, which is normalized to 1 at the maximum. The value of p_1 corresponding to the maximum of such a function is chosen as our best fitted value[3] and the CLs are determined by applying to this marginalized likelihood the conditions above on $\Delta\chi^2$ for $n_p = 1$.

In the course of the paper, for sake of simplicity we will report only the 68% CL for the listed best fitted parameters.

A. Temperature measurements (T)

To test the temperature evolution for the radiation component, we rely on the CMB temperatures derived from the absorption lines of high redshift systems and the ones from SZ effect in clusters of galaxies (we will collectively quote as T_{CMB}, hereafter). At high redshift the CMB temperature is recovered from the excitation of interstellar atomic or molecular species that have transition energies in the sub-millimetre range and can be excited by CMB photons. When the relative population of the different energy levels are in radiative equilibrium with the CMB radiation, the excitation temperature of the species equals that of the black-body radiation at that redshift, providing one of the best tools for determining the black-body temperature of the CMB in the distant Universe [27–34]. In Jetzer et al. [1], we adopted a sample of 5 QSO adsorption measurements, which is now updated to 9 after the recent measurements reported

[2] This is equivalent to a χ^2 minimization.

[3] Note that for asymmetric CLs, the χ^2 minimum and the maximum of the marginalized likelihood can be different.

in Noterdaeme et al. [24]. In summary we have 4 data points from the analysis of the fine structure of atomic carbon (AC) and 5 measurements based on the rotational excitation of CO molecules (CO) [24].

At lower redshift we use the measurements from the SZ effect. During passage through a cluster of galaxies some of the photons of the CMB radiation are scattered by electrons in the hot intracluster medium. This imprint was first described by SZ [35]. Thus, spectral measurements of galaxy clusters at different frequency bands yield independent intensity ratios for each cluster. The combinations of these measured ratios permit to extract the cosmic microwave background radiation (see Fabbri et al. [36]). We will rely on the data compilation in Luzzi et al. [23], which have analyzed the results of multifrequency SZ measurements toward several clusters from 5 telescopes (BIMA, OVRO, SUZI II, SCUBA and MITO).

We will match the observed T_{CMB} with the theoretical expression T_{th}, which we have derived in Eq. (2.33), by minimizing the following merit function

$$\chi^2_{TCMB} = \sum_{i=1}^{N_{TCMB}} \left(\frac{T^i_{th} - T^i_{CMB}}{\sigma_{CMB,i}} \right)^2 , \qquad (3.1)$$

where $\sigma_{CMB,i}$ is the error on the temperature estimates and $N_{TCMB} = 22$ is the number of available observational data.

B. High quality Supernovae Ia data set (SN)

The most important candle we use is the type Ia supernovae (SN). We adopt the UnionII dataset discussed in Amanullah et al. [37], which consists of $N_{SN} = 557$ datapoints from $z = 0$ to $z = 1.4$, compiled after the combination of different datasets and the consequent application of various selection cuts to create a homogeneous and high signal-to-noise sample.

The data points for SN are given in terms of distance modulus $\mu_{obs} = m - M$, where m and M are the apparent and absolute magnitude, respectively. The theoretical distance modulus is given by

$$\mu_{th}(z) = 5 \log_{10} D_L(z) + \mu_0 \ , \qquad (3.2)$$

where $\mu_0 = 42.38 - 5 \log_{10} h$ and $D_L(z)$ is the luminosity distance at the redshift z. The χ^2 function to be minimized is

$$\chi^2_{\rm SN} = \sum_{i=1}^{N_{SN}} \frac{(\mu_{th}(z_i) - \mu_{obs,i})^2}{\sigma^2_{SN,i}}, \qquad (3.3)$$

where $\sigma_{SN,i}$ is the error on $\mu_{obs,i}$. The parameter μ_0 is a nuisance parameter which depends on the Hubble constant. One can perform a standard marginalization on μ_0. Otherwise, following [38–41], it is easy to check that the χ^2 in Eq. (3.3) is equivalent to the following function

$$\tilde{\chi}^2_{\rm SN} = \tilde{A} - \frac{\tilde{B}^2}{\tilde{C}}, \qquad (3.4)$$

where

$$\tilde{A} = \sum_{i=1}^{N_{SN}} \frac{(\mu_{th}(z_i, \mu_0 = 0) - \mu_{obs,i})^2}{\sigma^2_{SN,i}} \ , \qquad (3.5)$$

$$\tilde{B} = \sum_{i=1}^{N_{SN}} \frac{(\mu_{th}(z_i, \mu_0 = 0) - \mu_{obs,i})}{\sigma^2_{SN,i}} \ , \qquad (3.6)$$

$$\tilde{C} = \sum_{i=1}^{N_{SN}} \frac{1}{\sigma^2_{SN,i}} \ . \qquad (3.7)$$

This new function does not depend on μ_0, allowing us to drop the contribution from the Hubble constant.

C. Baryon Acoustic Oscillation (A)

In the large-scale clustering of galaxies, the baryon acoustic oscillation signatures could be seen as a standard ruler providing the other important way to constrain the expansion history of the Universe. We use the measurement of the BAO peak from a spectroscopic sample of 46,748 luminous red galaxies (LRGs) observations of SDSS to test cosmology [42], which gives the value of $A = 0.469(n_s/0.98)^{-0.35} \pm 0.017$ at $z_{\rm BAO} = 0.35$ where $n_s = 0.96$ [43]. The expression of A can be written as

$$A = \frac{\sqrt{\Omega_{\rm m0}}}{(H(z_{\rm BAO})/H_0)^{\frac{1}{3}}} \left[\frac{1}{z_{\rm BAO}} \int_0^{z_{\rm BAO}} \frac{dz'}{H(z')/H_0} \right]^{\frac{2}{3}} \qquad (3.8)$$

which is evidently independent on H_0, and the relative χ^2 function is

$$\chi^2_{BAO} = \Big(\frac{A - 0.469(n_s/0.98)^{-0.35}}{0.017} \Big)^2 . \qquad (3.9)$$

D. CMB Data: the shift parameter (R)

The measurement of CMB anisotropies represents a powerful tool to constrain cosmological parameters, however, using the full data of CMB is time consuming, thus as an alternative it is common to rely on the measurement of the shift parameter R. The CMB shift parameter may provide an effective way to constrain the parameters of DE models since it has the very large redshift distribution, which allows to constrain the evolution of DE very well. The shift parameter R which is derived from the CMB data takes the form as

$$R \ = \ \sqrt{\Omega_{\rm m0}} \int_0^{z_{\rm CMB}} \frac{dz'}{H(z')/H_0}, \qquad (3.10)$$

where is $z_{\rm CMB} = 1090$ and the observed value for Eq. (3.10) has been updated to $R = 1.71 \pm 0.019$ from WMAP5 [43]. The χ^2 function is

$$\chi^2_{\rm CMB} = \Big(\frac{R - 1.71}{0.019} \Big)^2 . \qquad (3.11)$$

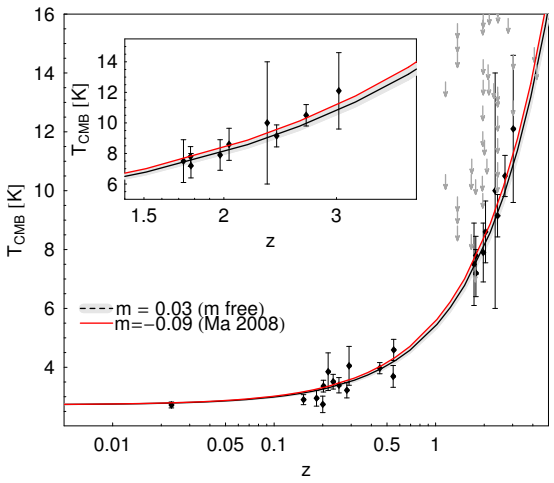

FIG. 2: Cosmic microwave background temperature as a function of the redshift. The black points with bars are the full collection of measurements from Luzzi et al. [23] and Noterdaeme et al. [24]. The gray arrows represent the upper limits derived from the analysis of atomic carbon (see [24] for details). The black line is the best fit result ($m = 0.03$), while the gray region is the 1σ uncertainty. The red line is the best fit recovered from Ma [20]. The inset panel show a magnified vision of the higher redshift region of the plot.

E. Observational $H(z)$ Data (OHD)

By using the differential ages of passively evolving galaxies determined from the Gemini Deep Deep Survey (GDDS) and archival data [44], Simon et al. determined H(z) in the range $0 < z < 1.8$ [45]. The 9 observational $H_{obs,i}$ datapoints can be obtained from [45–47]. The χ^2 statistics for these $H(z)$ data is

$$\chi^2_{\rm OHD} = \sum_{i=1}^{9} \frac{(\log_{10} H(z_i) - \log_{10} H_{obs,i})^2}{\sigma^2_{OHD,i}} \ , \qquad (3.12)$$

where $\sigma_{OHD,i}$ is the error on $\log_{10} H_{obs,i}$. Following the same procedure adopted in Sec.III B, to marginalize with respect to H_0, we replace the χ^2 in Eq. (3.12) with Eq. (3.4), where

$$\tilde{A} = \sum_{i=1}^{9} \frac{(\log_{10} H(z_i, H_0 = 1) - \log_{10} H_{obs,i})^2}{\sigma^2_{OHD,i}} \ , \qquad (3.13)$$

$$\tilde{B} = \sum_{i=1}^{9} \frac{(\log_{10} H(z_i, H_0 = 1) - \log_{10} H_{obs,i})}{\sigma^2_{OHD,i}} \ , \qquad (3.14)$$

$$\tilde{C} = \sum_{i=1}^{9} \frac{1}{\sigma^2_{OHD,i}} \ . \qquad (3.15)$$

IV. RESULTS

We discuss in this section the best fitted values for our model parameters. We first concentrate on the temperature-redshift relation, deriving constraints on both m and γ. In order to constrain the present matter density $\Omega_{\rm m0}$ and m we add the set of observational probes we have listed in the previous section, which are primarily linked to the Hubble parameter $H(z)$, and thus much more sensitive to matter component.

A. Constraints from $T(z) - z$ relation

As a primary test, following the same line in Jetzer et al. [1], we have compared the CMB temperature predicted (see Eq. (2.33)), with the updated collection of multi-redshift measurements of $T_{\rm CMB}$ we have discussed in the previous section. We set $T_0 = 2.725$ K, which is quite well determined in the literature [48], and the matter density $\Omega_{\rm m0} = 0.273$ to the value inferred in Komatsu et al. [43]. As we have shown in Sect. II D, the temperature is not sensitive to changes in $\Omega_{\rm m0}$ in the region where $\Omega_{\rm m0} \gtrsim 0.1 - 0.2$ in which it is constrained to lie from other probes. Thus, we are sure that our estimates are robust and in this section we will not discuss the constraints on $\Omega_{\rm m0}$ coming from the fitting of temperature-redshift relation. If we take $\gamma = 4/3$, then we find $m = 0.03^{+0.08}_{-0.09}$, which is lower than the estimated value of $m = 0.09 \pm 0.10$ in [1], but fully consistent within uncertainties, and also pretty consistent with $m = 0$. In Fig. 2 the temperature measurements (together with some upper limits) are shown, and our best fitted result is plotted and compared with the $m = -0.09$ result in Ma [20]. The value we have found corresponds to an effective equation of state $w_{\rm eff} = -0.99 \pm 0.03$, consistent with $w_{\rm eff} = -1$, and the transition redshift is $z_T = 0.78 \pm 0.08$. In order to check the impact of redshift distribution we separate the data in two redshift bins with $z < 0.6$ (SZ data only) and $z \geq 0.6$ (QSO adsorption lines only), finding the best fitted values $m = 0.12^{+0.12}_{-0.13}$ and $-0.05^{+0.12}_{-0.14}$, respectively. Although the uncertainties are very high and no statistically relevant conclusion can be reached, these results give some indications of a mild trend with lower redshift data preferring a DE decaying into matter and radiation, while data at $z > 0.6$ point to an opposite behavior. These results could be interpreted in a different way, in fact, the differences found could be due not to the different redshift coverage, but to some particular biases in the two kind of observations, SZ vs QSO adsorption lines. An indication of this suggestion comes if we divide the sample in three subsamples: 1) SZ data, 2) the data from the analysis of the fine structure of atomic carbon (AC), and 3) the measurements based on the rotational excitation of CO molecules in [24]. If we fit the model to the combined SZ+AC and SZ+CO samples we find $m = 0.11^{+0.11}_{-0.11}$ and $m = 0.03^{+0.09}_{-0.10}$, respectively. Because of the larger measurement errors,

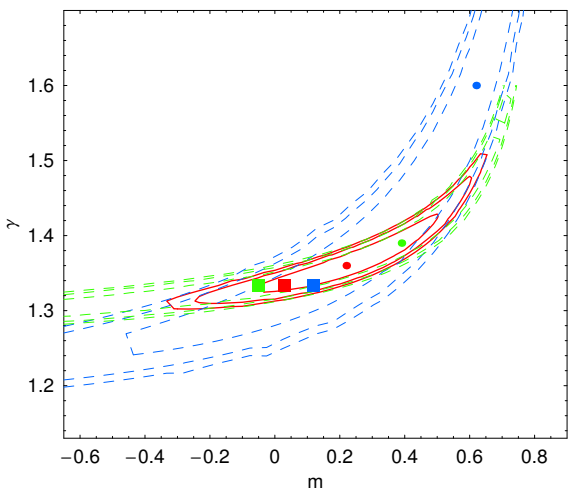

FIG. 3: The 68%, 90% and 95% confidence limit contours in the $m-\gamma$ plane from the fitting of temperature measurements. The red, blue and green contours are relative to the fit using all the sample, data for $z < 0.6$ and the ones for $z > 0.6$, respectively. The points are the best fitted values, while boxes are the results when $\gamma = 4/3$.

the AC data affect very little the results when only SZ measurements are adopted, and the result for the second sample shows that SZ and CO data mainly constrain m, and AC simply gives a tiny reduction on the errors. Of course, larger data samples would be needed to provide definitive answers.

Adopting a constant value for the ratio $\psi_\gamma/3n_\gamma H = \beta$ Lima et al. [17] have found the simple relation,

$$T(z) = T_0(1+z)^{1-\beta} \ . \tag{4.1}$$

If we fit all the sample we find $\beta = -0.002 \pm 0.03$, while for the low and high redshift subsamples we have $\beta = 0.06 \pm 0.08$ and -0.01 ± 0.03, respectively. These results are qualitatively consistent with what found in Noterdaeme et al. [24], and points to a similar trend as the one discussed above[4].

If γ is left free to change, we obtain the contours shown in Fig. 3. In all the redshift samples, for the best fitted value it turns out that $\gamma > 4/3$ and m is systematically more positive. Adopting the whole sample, the CL contours are broad, and from the marginalization with respect to the second parameter we find $\gamma = 1.35^{+0.03}_{-0.03}$ and $m = 0.25^{+0.23}_{-0.17}$, which corresponds to an effective equation of state $w_{\rm eff} = -0.92 \pm 0.07$ and the transition redshift is $z_T = 1.1 \pm 0.6$. When the two subsamples are adopted, wide confidence contours are found, particularly for the $z \geq 0.6$ sample, for which the contours at very low m are not closed. We obtain $\gamma = 1.3^{+0.2}_{-0.1}$ and $1.26^{+0.01}_{-0.01}$, while $m = 0.8^{+0.1}_{-0.3}$ and $0.6^{+0.1}_{-1.0}$, respectively for the low and high-z samples[5].

TABLE I: Maximum likelihood parameter and 1σ uncertainties of m for $\Omega_{\rm m0} = 0.273$ and for m and $\Omega_{\rm m0}$ when this last is left free to vary. The legend of the symbols is: T = Temperature, SN = Supernovae Ia, A = Baryon Acoustic oscillation parameter, R = Shift parameter, OHD = Observational $H(z)$ data.

Model	$\Omega_{\rm m0} = 0.273$	$\Omega_{\rm m0}$ free	
	m	$\Omega_{\rm m0}$	m
SN	$0.01^{+0.16}_{-0.17}$	$0.25^{+0.07}_{-0.09}$	$-0.2^{+0.6}_{-0.7}$
SN+T	$0.03^{+0.07}_{-0.08}$	$0.28^{+0.03}_{-0.02}$	$0.03^{+0.10}_{-0.08}$
SN+A	$0.01^{+0.16}_{-0.17}$	$0.28^{+0.02}_{-0.03}$	$0.03^{+0.19}_{-0.24}$
SN+A+R	$-0.04^{+0.03}_{-0.04}$	$0.27^{+0.02}_{-0.01}$	$-0.04^{+0.04}_{-0.04}$
SN+A+R+T	$-0.03^{+0.03}_{-0.03}$	$0.27^{+0.02}_{-0.01}$	$-0.03^{+0.03}_{-0.03}$
SN+A+OHD	$-0.03^{+0.14}_{-0.16}$	$0.27^{+0.03}_{-0.02}$	$-0.02^{+0.22}_{-0.18}$
SN+A+OHD+R	$-0.04^{+0.03}_{-0.04}$	$0.27^{+0.02}_{-0.01}$	$-0.04^{+0.03}_{-0.04}$

B. Constraints from independent measurements

If we set $\Omega_{\rm m0} = 0.273$, we can give some further constraints (shown in Table I) on m, using the other observational probes listed in Sect. III together with temperature measurements. We note that SNs alone are not able to constrain the value of m, producing very high uncertainties, also larger than the ones obtained using the temperature measurements alone. The Baryon Acoustic Oscillation parameter does not help, while temperature measurements will allow to reduce the uncertainties. These probes produce slightly positive values for m, while adding the Shift parameter and/or the $H(z)$ data give negative $m \sim -0.03, -0.04$. Anyway the uncertainties remain very large, with the only exception of the results when the Shift parameter is used in the fitting, m being in this case greatly constrained to $m = -0.04^{+0.03}_{-0.04}$. See Table I for details.

When $\Omega_{\rm m0}$ is left free to vary, we find the best fitted values and CL contours shown in Table I and Fig. 4. Remarkably, the best fitted values of $\Omega_{\rm m0}$ are perfectly in agreement with the values found in independent works [37, 43]. Consequently, it is not surprising that the re-

[4] Although we use the same datasample as in [24], we find some differences (although very minor), which could be possibly due to the way the asymmetric errors in QSO absorption line data are accounted for. In particular, we have adopted as error in the fit the average of the two errors.

[5] We notice that due to the particular form of the CL contours the best fit quantities derived from the maximum of the marginalized likelihood can be different from the χ^2 minimum. In fact, we find $\gamma = 1.6$ and 1.4, while $m = 0.6$ and $m = 0.4$ for the two subsamples, which differ from the ML values reported in the text, but consistent within errors, due to the large uncertainties.

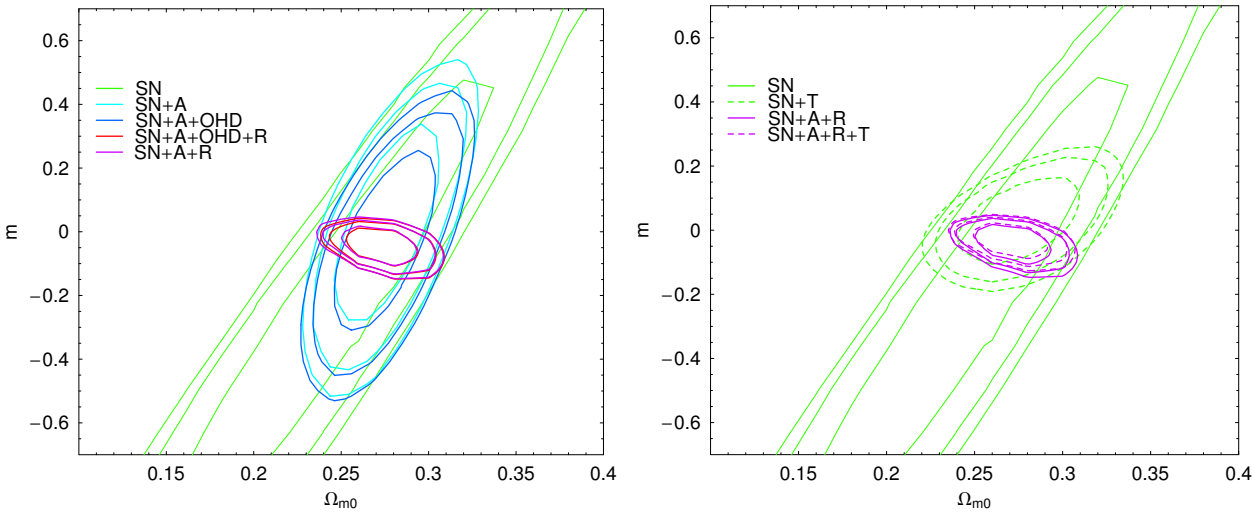

FIG. 4: The 68%, 90% and 95% confidence limit contours in the $\Omega_{\rm m0} - m$ plane. See the legends for the meaning of the symbols.

covered values for m, except for the case when only SNs are fitted, are still quite consistent with the estimates obtained when $\Omega_{\rm m0}$ is fixed (see Table I). If we consider the fit with SN+A+OHD+R, then our best fitted parameters correspond to an effective equation of state $w_{\rm eff} = -1.01 \pm 0.01$, in the phantom regime but fully consistent with $w_{\rm eff} = -1$, and the transition redshift is $z_T = 0.72 \pm 0.04$.

Adopting a standard DE model with an equation of state $p_x = w_x \rho_x$, and w_x free to vary, we have performed the fit, finding that $w_x \sim -1$, consistently with our results and still pointing to a cosmological constant as the best description for DE.

V. CONCLUSIONS

We have presented the properties of a variable DE model, following the approach in Jetzer et al. [1] (see also [15–18, 20]). The model relies on the assumption that the DE component is not conserved and exchanges particles with both DM and radiation components. In particular, we show that in order to have a viable model, DE needs to decay besides into radiation also in matter. Motivated by these considerations, we have concentrated the analysis on the case when only a small fraction is exchanged with radiation. We have dedicated particular attention to the thermodynamic properties of the model, discussing the theoretical relation between the radiation temperature and redshift and we have matched it to the most updated collection of CMB temperature measurements [1, 23, 24], consisting of both SZ data and high-redshift QSO adsorption line observations. First, we have constrained the model by setting $\gamma = 4/3$ and finding $m = 0.03^{+0.08}_{-0.09}$, consistent with our previous estimate within uncertainties, still consistent with the standard case of a $T \propto (1+z)$, i.e. with an effective equation of state $w_{\rm eff} = -1$. When γ is left free, then $m = 0.25^{+0.23}_{-0.17}$. Although the large contours indicate that is not possible to find statistically relevant departures from a standard cosmological constant, we find that a decaying DE, with an effective equation of state $w_{\rm eff} > -1$ is preferred. Then, for the first time, we test this kind of model combining both CMB temperature measurements and different observational data sets, like Supernovae Ia, CMB and large-scale structure data, etc. We find that $\Omega_{\rm m0}$ is almost independent on the combination of data we use, and in the best case is constrained to $\Omega_{\rm m0} = 0.27^{+0.02}_{-0.01}$. Moreover, while temperature measurements and SN data tend to furnish $m \gtrsim 0$, consistently with a decaying DE model, other datasets, like CMB data prefer the opposite situation with $m \lesssim 0$, i.e. a phantom-like model with $w_{\rm eff} < -1$.

Although the present data do not allow to find strong discrepancies with a classical cosmological constant model, we think that future surveys at high redshift could collect further measurements for CMB temperature, which could help us to further constrain the temperature-redshift relation. This kind of information, together with larger and higher quality samples of Supernovae and better CMB data or other standard candles like Gamma ray burst (GRBs) can allow to give independent constraints on both matter density $\Omega_{\rm m0}$ and effective equation of state $w_{\rm eff}$.

We notice that if DE does not decay into radiation (corresponding to $\epsilon = \tilde{\epsilon} = 0$ and thus m is no longer constrained) then the CMB temperature will scale in the standard way. Clearly, this would imply that if DE decays, this has to be into DM only. On the other hand a deviation of the CMB temperature from the standard scaling could be interpreted as DE decaying also into ra-

diation. In which case with Eq. (2.33) one can determine m and/or $\tilde{\epsilon}$ and thus get some insights on the decay mode of DE into radiation. Future data on the CMB temperature will allow to shed light on this important issue.

Acknowledgments

C. Tortora was supported by the Swiss National Science Foundation.

[1] P. Jetzer, D. Puy, M. Signore, C. Tortora, Gen. Relativ. Gravit., **43**, 1083 (2011)
[2] S. Perlmutter et al., Astrophys.J. **517**, 565 (1999)
[3] A.G. Reiss et al., Astron.J. **116**, 1009 (1998)
[4] P. de Bernardis et al., Nature **404**, 955 (2000)
[5] D.N. Spergel et al., Astrophys. J. Suppl. **170**, 377 (2007)
[6] R. Caldwell & M. Kamionkowski, Ann. Rev. Nucl. Part. Sci. **59**, 397 (2009)
[7] P.J.E. Peebles & B. Ratra, Astrophys. J. Lett. **325**, L17 (1988)
[8] B. Ratra & P.J.E. Peebles, Phys. Rev. D **37**, 3406 (1988)
[9] V. Sahni & A.A. Starobinsky, Int. J. Mod. Phys. **D9** 373 (2000)
[10] R.R. Caldwell, Phys. Lett. B **545**, 23 (2002)
[11] T. Padmanabhan, Phys. Rep. **380**, 235 (2003)
[12] P. J. E. Peebles and B. Rathra, Rev. Mod. Phys. **75**, 559 (2003)
[13] M. Demianski, E. Piedipalumbo, C. Rubano, C. Tortora, A&A **431** 27D (2005)
[14] V. F. Cardone, C. Tortora, A. Troisi, and S. Capozziello, Phys. Rev. **D73**, 043508 (2006)
[15] J.A.S. Lima, Phys. Rev. D. 54, 2571 (1996)
[16] J.A.S. Lima and J.S. Alcaniz, Astron. and Astrophys. **348**, 1 (1999)
[17] J.A.S. Lima, A.I. Silva and S.M. Viegas, Mon. Not. R. Astron. Soc. 312, 747 (2000)
[18] D. Puy, Astron. and Astrophys. **422**, 1 (2004)
[19] W. Chen, Y.S. Wu, Phys. Rev. D 41 (1990) 695; W. Chen, Y.S. Wu, Phys. Rev. D 45 (1992) 4728, Erratum.
[20] Y. Ma, Nucl. Phys. B **804**, 262 (2008)
[21] S. Weinberg, *Gravitation and Cosmology: Principles and Applications of the General Theory of Relativity* (Wiley, New York, 1972!.
[22] E.S. Battistelli et al., Astrophys. J. **580**, L101 (2002)
[23] G. Luzzi, M. Shimon, L. Lamagna, Y. Rephaeli, M. De Petris, A. Conte, S. De Gregori and E. Battistelli, Astrophys. J. **705**, 1122 (2009)
[24] P. Noterdaeme, P. Petitjean, R. Srianand, C. Ledoux, and S. López, A&A **526**, L7 (2011)
[25] M. Jamil, E.N. Saridakis and M.R. Setare, Phys. Rev. **D 81**, 023007 (2010)
[26] J.C. Mather et al., Astrophys. J. 512, 511 (1999).
[27] J. Ge, J. Bechtold and J. Black, Astrophys. J **474**, 67 (1997)
[28] R. Srianand, P. Petijean and C. Ledoux, Nature **408**, 931 (2000)
[29] P. Molaro, S. Levshakov, M. Dessauges-Zavadsky and S. D'Odorico, Astron. and Astrophys. **381**, L64 (2002)
[30] D. Puy, G. Alecian, J. Leorat, J. Lebourlot and G. Pineau des Forets, Astron. and Astrophys. **267**, 337 (1993)
[31] D. Galli and F. Palla, Astron. and Astrophys. **335**, 403 (1998)
[32] P. Stancil, S. Lepp and A. Dalgarno, Astrophys. J. **509**, 1 (1998)
[33] J. Cui, J. Bechtold, J. Ge and D. Meyer, Astrophys. J. **633**, 649 (2005)
[34] R. Srianand, P. Noterdaeme, C. Ledoux and P. Petijean, Astron. and Astrophys. **482**, L39 (2008)
[35] R. Sunyaev and Y. Zel'dovich, Comm. Ap. Sp. Phys.**4**, 173 (1972)
[36] R. Fabbri, F. Melchiorri and V. Natale, Astrophys. Sp. Sci. **59**, 223 (1978)
[37] R. Amanullah et al., Astron. Astrophys. bf 486, 375 (2008)
[38] E. Di Pietro, J.F. Claeskens, Mon. Not. Roy. Astron. Soc. **341**, 1299 (2003)
[39] S. Nesseris, L. Perivolaropoulos, Phys. Rev. D **72**, 123519 (2005)
[40] L. Perivolaropoulos, Phys. Rev. D **71**, 063503 (2005)
[41] H. Wei, PhLB, **687**, 286 (2010)
[42] D.J. Eisenstein, et al., Astrophys. J. **633** 560 (2005)
[43] E. Komatsu et al., Astrophys. J. Suppl. **180**, 330 (2009)
[44] R. G. Abraham et al. [GDDS Collaboration], Astron. J. **127**, 2455 (2004)
[45] J. Simon, L. Verde, R. Jimenez, Phys. Rev. D **71** 123001 (2005)
[46] L. Samushia and B. Ratra, Astrophys. J. **650**, L5 (2006)
[47] H. Wei and S.N. Zhang, Phys. Lett. B **644**, 7 (2007)
[48] J.C. Mather et al., Astrophys. J. **512**, 511 (1999)